Inorganic Chemistry

Article

pubs.acs.org/IC

Platinum(II) Complexes of N^C^N-Coordinating 1,3-Bis(2-pyridyl)benzene Ligands: Thiolate Coligands Lead to Strong Red Luminescence from Charge-Transfer States

William A. Tarran,[†] Gemma R. Freeman,[†] Lisa Murphy,[†] Adam M. Benham,[‡] Ritu Kataky,[†] and J. A. Gareth Williams*[,†]

[†]Department of Chemistry, Durham University, Durham DH1 3LE, U.K.

[‡]School of Biological and Biomedical Sciences, Durham University, Durham DH1 3LE, U.K.

Supporting Information

ABSTRACT: A new family of platinum(II) complexes of the form PtL^{n}SR have been prepared, where L^n represents a cyclometalating, N^C^N-bound tridentate ligand and SR is a monodentate thiolate ligand. The complexes fall into two groups, those of PtL^{1}SR where HL^1 = 1,3-bis(2-pyridyl)-benzene, and those of PtL^{2}SR, where HL^2 = methyl 3,5-bis(2-pyridyl)benzoate. Each group consists of five complexes, where R = CH_3, C_6H_5, p-C_6H_4-CH_3, p-C_6H_4-OMe, p-C_6H_4-NO_2. These compounds, which are bright red, orange, or yellow solids, are formed readily upon treatment of PtL^{n}Cl with the corresponding potassium thiolate KSR in solution at room temperature. The replacement of the chloride by the thiolate ligand is accompanied by profound changes in the photophysical properties. A broad, structureless, low-energy band appears in the absorption spectra, not present in the spectra of PtL^{n}Cl. In the photoluminescence spectra, the characteristic, highly structured phosphorescence bands of PtL^{n}Cl in the green region are replaced by a broad, structureless emission band in the red region. These new bands are assigned to a $\pi_S/d_{Pt} \rightarrow \pi^*_{N^C^N}$ charge-transfer transition from the thiolate/platinum to the N^C^N ligand. This assignment is supported by electrochemical data and TD-DFT calculations and by the observation that the decreasing energies of the bands correlate with the electron-donating ability of the substituent, as do the increasing nonradiative decay rate constants, in line with the energy-gap law. However, the pair of nitro-substituted complexes do not fit the trends. Their properties, including much longer luminescence lifetimes, indicate that the lowest-energy excited state is localized predominantly on the arenethiolate ligand for these two complexes. Red-emitting thiolate adducts may be relevant to the use of PtL^{n}Cl complexes in bioimaging, as revealed by the different distributions of emission intensity within live fibroplast cells doped with the parent complex, according to the region of the spectrum examined.

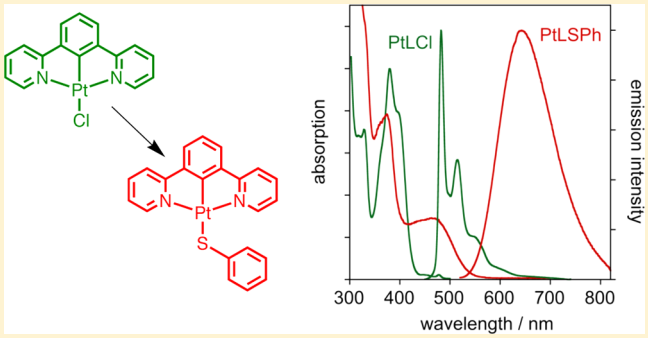

INTRODUCTION

The development of brightly photoluminescent platinum(II) complexes has been driven over the past 15 years by a number of emerging applications, such as triplet-harvesting phosphors for light-emitting devices,[1] emissive units for chemosensing,[2] probes for biological molecules, including nucleic acids and proteins,[3] and bioimaging agents.[4] Cyclometalated complexes of ligands featuring a combination of aryl and heterocyclic rings that bind through a partnership of C and N atoms have been featured in many studies.[5] These ligands are typically both good σ-donors, by virtue of the metalated carbon atom in particular, and good π acceptors through the coordinated heterocycle. Consequently, they are strong-field ligands that lead to large separations between the highest occupied and vacant d orbitals. This feature ensures that metal-centered excited states—which are highly antibonding and therefore strongly deactivating—are displaced to higher energy, making it more likely that lower-energy states (e.g., those of metal-to-ligand charge-transfer or ligand-centered character) can emit efficiently.[6]

Most cyclometalated platinum(II) complexes studied to date have employed bidentate ligands such as 2-phenylpyridine (ppy) and derivatives thereof, and indeed, such complexes are frequently quite strongly luminescent.[5] Nevertheless, bis-bidentate complexes are potentially susceptible to a distortion away from square planarity toward a D_{2d} geometry in the excited state, and such distortions may facilitate nonradiative decay, imposing a limit on the luminescence efficiency.[7] The use of tridentate and tetradentate analogues can lead to more rigid complexes and hence to brighter emission. In particular, the platinum(II) complex of N^C^N-coordinated 1,3-bis(2-pyridyl)benzene (PtL^{1}Cl; Scheme 1) has a luminescence quantum yield of 0.6 in solution at room temperature,[8] 1

Received: March 11, 2014
Published: May 21, 2014

   dx.doi.org/10.1021/ic500555w | Inorg. Chem. 2014, 53, 5738−5749

Scheme 1. Synthesis of the Two Series of Thiolate Complexes PtL^{n}SAr from the Parent Chloro Complexes PtL^{n}Cl (n = 1, 2)[a]

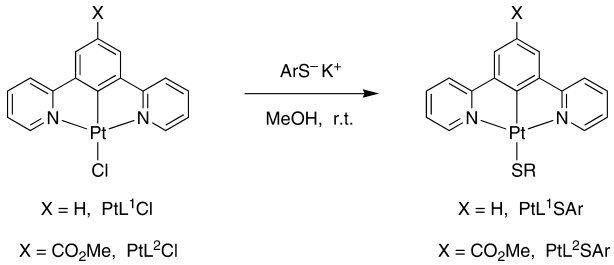

[a]The methanethiolate complexes were prepared similarly, but using an aqueous solution of NaSMe.

order of magnitude higher than that of its bidentate cousin Pt($N^\wedge$C-ppy)(N-ppyH)Cl[9] or its N^N^C-coordinated isomer,[10] despite the individual ligating units being identical.[11] Moreover, the excited-state energy and hence color of such tridentate complexes can be tuned over a wide range through the introduction of substituents into the aryl or pyridyl rings, without substantially compromising the quantum yields.[12] The low molecular weights and charge neutrality of these complexes render them attractive for incorporation as triplet-harvesting phosphors into vacuum-sublimed or spin-coated OLEDs, and devices with impressive performance characteristics have been obtained.[13]

There remain rather few platinum(II) complexes that emit efficiently in the red region of the spectrum.[1e] Typically, the quantum yields of red-emitting complexes tend to be limited not by the energetic proximity of d−d states (problematic for blue emitters) but by increased nonradiative deactivation through intramolecular transfer of electronic energy into vibrational energy. The so-called "energy-gap law"—which describes the increase in nonradiative decay with decreasing excited-state energy[14]—has been found to hold quite well for many series of metal complexes,[15] including some of platinum(II).[16,17]

One approach to obtaining red platinum(II)-based emitters relies on the formation of excimers or aggregates, either intermolecular or intramolecular, where two Pt units are brought in close proximity and are able to interact, normally in a face-to-face manner in such a way as to stabilize the excited state.[18] More recently, it has been shown that the presence of a second metal ion in dinuclear Pt(II) complexes with bridging cyclometalating ligands (e.g., those based on 4,6-diphenylpyrimidine and 2,3- and 2,5-diphenylpyrazine) also leads to significant red shifts while retaining high quantum yields.[19] In both of these strategies for obtaining red emission, however, two or more metal centers are evidently required.

The present work deals with the synthesis and the photophysical and electrochemical characterization of two new series of mononuclear N^C^N-coordinated platinum(II) complexes, related to PtL^{1}Cl and its 4-methyl ester analogue PtL^{2}Cl (Scheme 1), but in which the monodentate chloride coligand is replaced by a thiolate. Previously, we have found that the replacement of chloride in PtL^{1}Cl by ligands such as pyridines, methoxide, arylphosphines, and isothiocyanate has relatively little effect on the excited-state energy.[20,21] Other researchers have likewise found that phenols and acetylides do not have large effects on the emission energies.[13a,12d,22] This can be rationalized quite readily with the aid of TD-DFT calculations, which reveal that the lowest-energy triplet excited state on PtL^{1}Cl is largely localized on the dipyridylbenzene, albeit with sufficient metal contribution to promote the formally forbidden radiative process.[23] The coligand apparently makes only a relatively minor contribution to the frontier orbitals involved in the excitation. Here, we show that the introduction of methanethiolate (MeS^-) or a range of arenethiolates (ArS^-) into the coordination sphere of the platinum ion has a profound influence on the excited-state energy, strongly shifting the emission to the red region. A combination of electrochemical measurements and TD-DFT calculations allows the origins of the effect to be traced to a fundamental change in the nature of the excited state when the chloride ligand is replaced by a more electron rich sulfur atom.

RESULTS

Synthesis of Complexes. The 10 new complexes produced and studied in this work are shown in Figure 1.

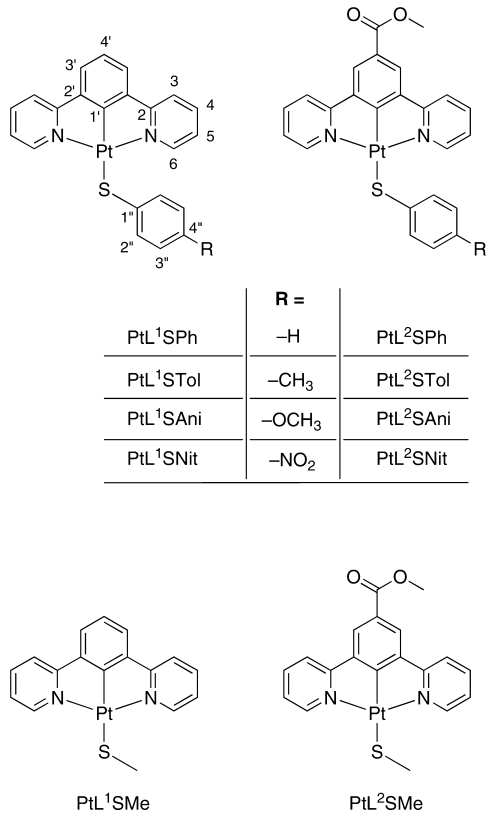

Figure 1. Structural formulas of the 10 new thiolate complexes prepared in this work.

The arenethiolate complexes PtL^{n}SAr (n = 1, 2; Ar = C_6H_5, p-$C_6H_4CH_3$, p-C_6H_4OMe, p-$C_6H_4NO_2$) were readily prepared from the parent chloro complexes PtL^{1}Cl and PtL^{2}Cl by addition of a solution of the respective potassium thiolate ArS^-K^+ in methanol at room temperature, itself prepared immediately before use from the corresponding thiol ArSH by treatment with potassium *tert*-butoxide (Scheme 1). The thiolate complexes precipitated from solution as yellow, orange, or red solids. Successive washing of the solids with water, methanol, and diethyl ether led to analytically pure samples of the desired complexes. Even upon treatment with the thiol itself, without prior addition of base, partial conversion of the starting chloro complexes to the thiolate derivatives was

dx.doi.org/10.1021/ic500555w | Inorg. Chem. 2014, 53, 5738−5749

Table 1. Ground-State UV−Visible Absorption and Electrochemical Data of the Platinum(II) Thiolate Complexes in CH_2Cl_2 Solution at 298 K

complex	absorption λ_{max}/nm[a] (ε/M^{-1} cm^{-1})	$E_{1/2}^{red}$/V[b] (Δ/mV)	E_p^{ox}/V[b]	$E_p^{ox} - E_{1/2}^{red}$/V
PtL^1SMe	234 (33700), 261 (31000), 290 (21300), 307 (13700), 332 (7490), 365 (5660), 377 (5980), 465 sh (2210)	−1.36	−0.36	1.00
PtL^1SPh	236 (36400), 261 (35100), 282 (31300), 289 (31800), 306 sh (18500), 332 sh (8300), 363 (6420), 376 (6510), 452 sh (2040)	−1.39 (240)	−0.03	1.36
PtL^1STol	236 (30100), 261 (29300), 280 (25700), 288 (25600), 306 sh (14700), 330 sh (7500), 363 (5700), 377 (5990), 460 sh (1820)	−1.36 (220)	−0.10	1.26
PtL^1SAni	237 (41600), 262 (41400), 290 (32700), 306 (19400), 330 sh (10600), 365 (7490), 377 (7580), 463 sh (2450)	[c]	−0.12	
PtL^1SNit	237 (35200), 258 (33000), 288 (24300), 305 (15500), 335 (8950), 376 sh (11000), 415 (17100), 455 sh (13600)	−1.36, −1.73 (160)	+0.26	1.62
PtL^2SMe	264 (54600), 285 (34000), 307 (19800), 330 sh (11600), 369 (6690), 468 (3250)	[c]	−0.35	
PtL^2SPh	266 (61600), 285 (45700), 305 (23600), 330 sh (12200), 360 (7350), 373 (7780), 465 (2890)	−1.44 (290)	−0.07	1.37
PtL^2STol	266 (58400), 306 (21300), 332 sh (11100), 362 (7380), 375 (7820), 469 (2720)	−1.38 (280)	−0.11	1.27
PtL^2SAni	265 (60100), 307 (21000), 332 sh (11600), 362 (7490), 376 (7660), 472 (3150)	−1.43 (250)	−0.22	1.21
PtL^2SNit	262 (31500), 305 (17000), 333 sh (8030), 378 (11500), 415 (17800), 455 sh (13800)	−1.45 (200), −1.87 (90)	+0.13	1.58

[a]Corresponding data for PtL^1Cl: 238 (33000), 256 (25800), 277 (20400), 290 (21100), 332 (6510), 380 (8690), 401 (7010), 454 (270), 485 (240). For PtL^2Cl: 329 (7560), 380 (9990), 397 (7880), 446 (180), 478 (200). [b]Using Bu_4NPF_6 (0.1 M) as the supporting electrolyte. Peak potentials are given for the oxidations, all of which were irreversible, and for those reductions where the return wave was ill-defined. For reductions showing return waves, the quoted values refer to $E_{1/2}$ and the peak-to-peak separation is given in parentheses. Values refer to a scan rate of 100 mV s^{-1} and are quoted relative to $Fc^+|Fc$. [c]The reduction wave was poorly defined for this complex.

observed. However, a substantial quantity of PtL^nCl starting material remained in this case, which proved to be difficult to separate from the products. The methanethiolate complexes PtL^nSMe were similarly prepared by addition of aqueous sodium methanethiolate to PtL^nCl suspended in methanol.

The identity of the new complexes was confirmed by ^1H NMR spectroscopy, mass spectrometry, and elemental analysis. The atom-numbering scheme for the ^1H NMR assignments is shown in Figure 1. The ^1H NMR spectra of the arenethiolate complexes displayed a pattern of resonances similar to that of the parent chloro complexes, with the additional set of expected aromatic signals due to the aryl ring of the thiolate. In the case of PtL^nSTol, a weak coupling in the COSY spectrum between the tolyl methyl group and $H^{3''}$ allowed unambiguous assignment of the two pairs of doublets in the thiolate aryl ring, that nearest the sulfur atom resonating at higher frequency. The use of conventional electron beam ionization (EI) mass spectrometry proved to be surprisingly successful at identifying the desired products, revealing the molecular ion for each arenethiolate complex, together with some fragmentation peaks (e.g., loss of thiolate, loss of CO_2Me in the L^2 series, tropylium ion in the tolyl complexes). In contrast, electrospray (ES) mass spectrometry generally failed to detect the molecular ion, M^+, although a number of cluster species were observed. Mass and isotope patterns indicated various dimetallic clusters incorporating complete or partially fragmented thiols. A feature common to several of the ES mass spectra recorded was the appearance of a pair of cluster ions comprising two Pt(N^C^N) units and one intact thiolate (RS) either with or without an additional sulfur atom. It is likely that these species involve bridging sulfurs between two Pt centers, and indeed, in the chemistry of related platinum terpyridyl complexes, sulfur-bridged species such as $\{[Pt(tpy)]_3S\}$ have been unambiguously characterized by X-ray diffraction.[24] The ES mass spectrum of PtL^1SMe showed a series of peaks representing $[3M]^+$, $[3M - Me]^+$, $[3M - 2Me]^+$, and $[3M - 3Me]^+$. A likely structure of the gas-phase species formed that would lead to such a pattern is a ring comprising three Pt(N^C^N) units bridged by SMe units. Also present in some spectra were more conventional clusters such as $[2M + Na]^+$ and $[3M + Na]^+$.

In the solid state, the thiolate complexes are indefinitely stable: no decomposition has been observed over a period of 9 years. In solution, however, the compounds degrade at a rate that varies significantly with the solvent. In d_3-acetonitrile, for example, new sets of peaks begin to appear in the ^1H NMR spectra over a period of several minutes. This degradation also occurs in degassed solutions. The process is slower in dichloromethane, allowing some physicochemical characterization to be achieved in this solvent (see below). Of the common solvents tested, the stability appears to be highest in d_6-dimethyl sulfoxide. The identity of the decomposition products remains somewhat elusive, but the process probably involves decoordination of the thiolate facilitated by the well-known high trans effect of cyclometalated carbon atoms. van Eldik and co-workers have previously studied the rate of displacement of chloride from Pt(N^C^N)Cl by nucleophiles and found that the reactivity may be 10^3−10^4 times higher than that of isomeric Pt(N^N^C)Cl complexes.[25]

Electrochemistry of the Complexes and Frontier Orbital Description. The ground-state redox potentials of the complexes were measured by cyclic voltammetry in dichloromethane solution, in the presence of Bu_4NPF_6 (0.1 M) as the supporting electrolyte. Data are reported in Table 1 relative to the ferrocene|ferrocenium couple ($Fc|Fc^+$) under the same conditions. All of the complexes display an irreversible but well-defined oxidation wave, in the region −0.4 to +0.3 V. In all cases, the oxidation is cathodically shifted—occurring at less positive/more negative potentials—in comparison to the parent chloro complexes (E_p^{ox} = +0.35 and +0.39 V for PtL^1Cl and PtL^2Cl, respectively). Among the four arenethiolate complexes of a given L^n, the trend in oxidation potentials (i.e., R = OMe < Me < H < NO_2) qualitatively reflects the electron-donating character of the thiolate substituent (i.e., R = OMe > Me > H > NO_2). The two methanethiolate complexes, PtL^nSMe, are the most readily oxidized complexes, with E_p^{ox} values around −0.35 V. For the two series PtL^1SAr and PtL^2SAr, it is seen that those of L^2 are slightly shifted

dx.doi.org/10.1021/ic500555w | Inorg. Chem. 2014, 53, 5738−5749

cathodically in comparison to their L^1 counterparts, although the differences are small.

All of the arenethiolate complexes display a first reduction wave at around −1.40 V (the potentials are within 50 mV of this value in each case; Table 1). This process is partially reversible at higher scan rates, with a peak-to-peak separation of around 200−300 mV. At lower scan rates, typically <100 mV s^{-1}, the return wave becomes poorly defined.

Pioneering studies by Eisenberg and co-workers[26] and by Weinstein and colleagues[27] have previously examined complexes of the form Pt(N^N)(S^S), where N^N represents a diimine ligand such as bipyridine and S^S a chelating dithiolate or a pair of monodentate thiolate ligands. These provide an interesting point of comparison with the present systems. They too typically display an irreversible oxidation process and one or two reversible or partially reversible reduction processes. Similar results have been reported for terpyridyl analogues of the form $[Pt(N^N^N)SR]^+$.[28] Detailed studies involving techniques such as EPR and resonance Raman spectroscopy, in conjunction with TD-DFT calculations, have indicated that the reduction is based primarily on the diimine (or triimine) ligand, while the oxidation involves the metal and the thiolate ligands.[29,27] Similar conclusions are made in the present case, as discussed in the sections that follow.

UV−Visible Absorption Spectra. The replacement of the chloride ligand in PtL^nCl by the thiolates has a striking effect on the absorption, as is immediately evident during the syntheses: the products have intense red, orange, and yellow colors, in contrast to the pale yellow of the starting materials. The spectral origin of the observed change is highlighted in Figure 2, where the absorption spectrum of PtL^2SPh (used as a representative model for the thiolate complexes) is shown together with that of its parent chloro complex PtL^2Cl. The two complexes have in common a set of intense bands in the far-UV (λ <300 nm). They also both feature a band at around 375 nm, of fairly similar intensity. However, while the longest-wavelength, spin-allowed band in PtL^2Cl is a shoulder at 400 nm, PtL^2SPh displays a well-defined, intense, broad band centered at around 465 nm, $\varepsilon \approx 3000$ M^{-1} cm^{-1}, for which there is no counterpart in PtL^2Cl (note that the very weak, sharp bands at 446 and 478 nm in PtL^2Cl are spin-forbidden excitations to triplet ligand-centered states[8]).

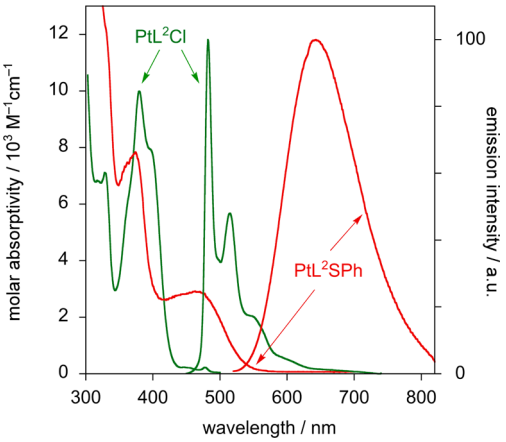

Figure 2. Absorption and emission spectra of PtL^2Cl (green lines) and PtL^2SPh (red lines) in CH_2Cl_2 at 298 K.

The UV−visible spectra of all five PtL^2SR complexes are shown in Figure 3a, and numerical data are compiled in Table 1. It can be seen that the spectra of PtL^2STol and PtL^2Ani are very similar to that of PtL^2SPh, with a small shift of the long-wavelength band toward the red, in the λ_{max} order phenyl < tolyl < anisyl. The spectrum of PtL^2SMe is also very similar. In contrast, the spectrum of PtL^2SNit is strikingly different in the region λ >350 nm, displaying a very intense band at 415 nm (ε = 17800 M^{-1} cm^{-1}), on which are superimposed bands at 378 and 455 nm which may correspond to those seen at such wavelengths in the other four thiolate complexes.

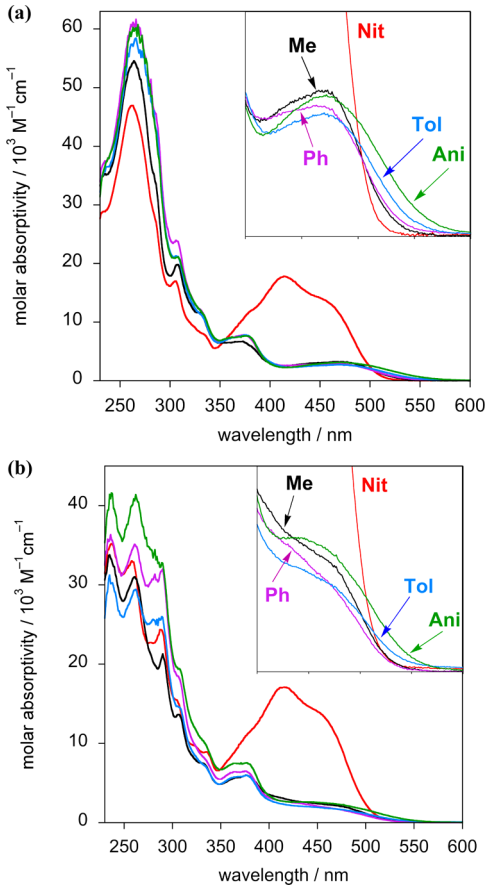

Figure 3. (a) Absorption spectra of PtL^2SR complexes in CH_2Cl_2 at 298 K (the inset shows an expansion of the region of the low-energy bands around 465 nm) and (b) the corresponding spectra of PtL^1SR complexes.

An essentially identical picture emerges from the spectra of the corresponding complexes of L^1 (Figure 3b), the spectrum of the nitro complex again being very different from those of the other four complexes. In this case, the long-wavelength band in each of the phenyl, tolyl, anisyl, and methyl complexes is slightly blue-shifted in comparison to its L^2 counterpart, and the overlap with the higher-energy bands renders it more of a shoulder than a clear-cut band.

The appearance of the long-wavelength band in the region 452−472 nm that accompanies the change from chloride to thiolate can be rationalized in terms of a new, low-energy charge-transfer state, as observed in the related diimine complexes referred to above.[26−29] The electron-rich sulfur atoms are expected to lead to a HOMO that will span the thiolate and the metal atom, in contrast to the parent chloride

dx.doi.org/10.1021/ic500555w | Inorg. Chem. 2014, 53, 5738−5749

complex, where the most electron rich part of the molecule comprises the metal and cyclometalating aryl ring.[23] Meanwhile, the LUMO can be expected to remain localized largely on the pyridyl rings of the N^C^N ligand. A low-energy excited state of $d_{Pt}/\pi_{RS} \rightarrow \pi^*_{NCN}$ character may thus be anticipated, and indeed, such a conclusion is supported by time-dependent density functional theory calculations (vide infra).

Further support for such an assignment comes from the variation in λ_{max} with substituent, either in the aryl ring of the thiolate or in the N^C^N ligand. Thus, the red shift in the L^2 complexes versus those with the corresponding thiolate in the L^1 series can be understood in terms of the electron-withdrawing influence of the ester group slightly stabilizing the N^C^N-based LUMO. Meanwhile, the order of λ_{max} phenyl < tolyl < anisyl is attributed to the effect of the increasingly electron-donating substituent in destabilizing the HOMO. Indeed, although the differences between the λ_{max} values are small, there appears to be a correlation of the absorption energy with $|E^{ox} - E^{red}|$ (Figure 4), consistent with the notion that the

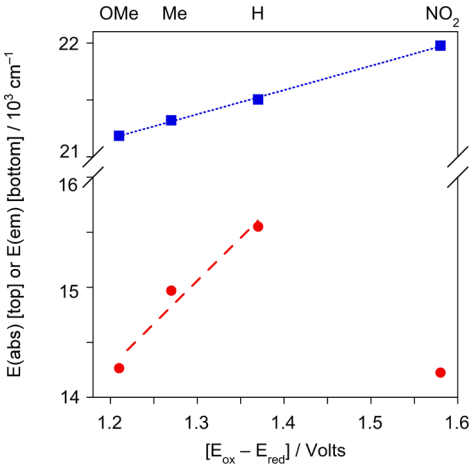

Figure 4. Energy of absorption (top) and emission (bottom) versus the difference between the oxidation and reduction potentials of PtL^2SR. The blue dotted line through the absorption data points represents the linear best fit for all four complexes (gradient 2100 cm^{-1}/V). The red dashed line for the emission data represents the best fit for the phenyl, tolyl, and anisyl complexes, *excluding* the nitro analogue (gradient 7800 cm^{-1}/V).

orbitals involved in the excitation are similar to those ionized and populated through electrochemical oxidation and reduction, respectively.

Charge-transfer excited states frequently give rise to significant solvatochromism, if the redistribution of electron density in the excited state is noncentrosymmetric, as in this instance. The limited solubility of the compounds and the propensity to degradation in some solvents hampers a detailed investigation, but using as an example PtL^2SPh in four solvents of differing polarity, it can be seen that there is significant negative solvatochromism in the low-energy absorption band (see Figure S1 and Table S1 in the Supporting Information). The λ_{max} value shifts from 494 nm in toluene to ~453 nm in acetonitrile, a destabilization of around 1800 cm^{-1}.

Finally, the much more intense band that appears around 415 nm in the complexes containing the nitro-substituted thiolate ligand can be attributed to a strongly allowed intraligand charge-transfer (ILCT) transition within the 4-nitrobenzenethiolate ligand, i.e., $\pi(SC_6H_4) \rightarrow \pi^*(NO_2)$, akin to that responsible for the well-known color of the 4-nitrophenolate anion. Similarly intense bands in this region have been observed previously in complexes incorporating this ligand both with Pt(II)[27a] and with other metal ions.[30] Notably, this band shows little solvatochromism (as exemplified by the spectra of PtL^2SNit in different solvents, Figure S2 (Supporting Information)), in line with a more limited and localized redistribution of the electron density in the molecule. TD-DFT calculations support this assignment (see Time-Dependent Density Functional Theory (TD-DFT) and Interpretation of Emission Data below).

Photoluminescence. *Experimental Observations.* All of the new complexes are luminescent in solution upon UV/blue-light excitation, emitting in the red region of the spectrum. Reference to Figure 2 once again makes clear the profound effect of the substitution of chloride by thiolate on the emission spectrum. Whereas the chloro complex PtL^2Cl displays vibronically structured bands in the green region (λ_{0-0} 481 nm) with a luminescence lifetime of 8 μs, the emission of PtL^2SPh is shifted far to the red (λ_{max} 643 nm) and comprises a broad, unstructured band with a lifetime that is 1 order of magnitude shorter (τ = 880 ns). The luminescence quantum yield is 0.16. Although it is lower than that of the parent chloro complex, it should be noted that *this value is exceptionally high for such a deeply red emitting mononuclear Pt(II) complex.* Quantum yields of red phosphors are invariably compromised by increased nonradiative decay processes, a point returned to in more detail below. The complex PtL^1SPh displays similar emission characteristics (λ_{max} 634 nm; τ = 770 ns; Φ = 0.17).

The intensity-normalized emission spectra of the family of five PtL^2SR complexes are shown in Figure 5a and those of PtL^1SR in Figure 5b. The emission maxima, luminescence lifetimes, and quantum yields are compiled in Table 2. A number of trends emerge from these data.

(i) For a given thiolate ^-SR, the emission maximum is red-shifted for PtL^2SR in comparison to PtL^1SR, with the exception of the pair of nitro-substituted complexes, where the order is reversed.

(ii) For both series of arenethiolate complexes (n = 1, 2), the emission maxima are increasingly red-shifted in the λ_{max} order $PtL^nSPh < PtL^nSTol < PtL^nSAni < PtL^nSNit$. For the first three complexes in the PtL^2SAr series, there is a convincing linear correlation between the emission energy and $|E^{ox} - E^{red}|$, but the nitro-substituted complex clearly does not follow the trend (Figure 4). The best fit line through the data points for the complexes *excluding* the nitro-substituted compound gives a gradient of 7800 cm^{-1}/V.

(iii) For both series of arenethiolate complexes, the luminescence lifetime of the nitro-substituted complex is much longer than those of the other three complexes. The lifetimes of PtL^1SNit and PtL^2SNit are 7.4 and 11.3 μs, respectively, whereas all the other complexes have lifetimes <1 μs. Among the other complexes, the order of luminescence lifetimes for both series (n = 1, 2) is $PtL^nSPh > PtL^nSTol > PtL^nSAni$.

(iv) The luminescence quantum yields in both series also follow the order $PtL^nSPh > PtL^nSTol > PtL^nAni$, as observed for the lifetimes. The nitro-substituted complexes have small quantum yields, similar to those for the anisyl-subtituted analogues, despite their long lifetimes.

(v) The spectrum of PtL^2SMe is essentially identical with that of PtL^2SPh, and likewise the spectrum of PtL^1SMe is similar to that of PtL^1SPh. However, the methanethiolate

dx.doi.org/10.1021/ic500555w | Inorg. Chem. 2014, 53, 5738−5749

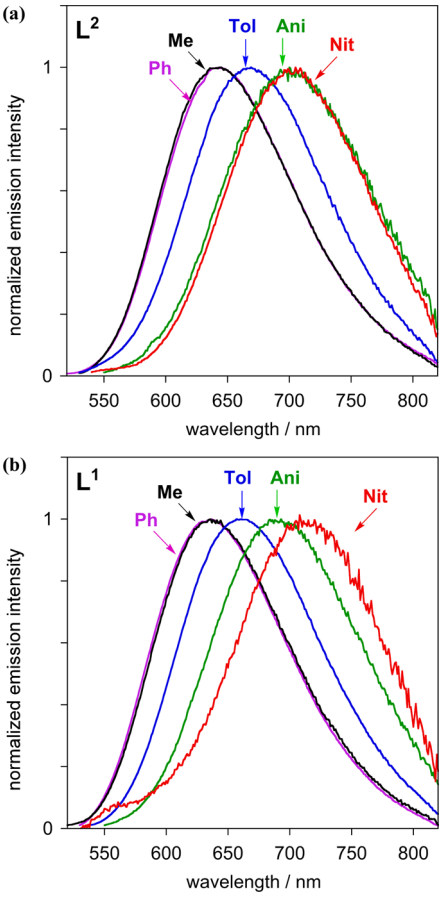

Figure 5. (a) Emission spectra of PtL^{2}SR complexes in degassed CH_2Cl_2 at 298 K and λ_{ex} = 460 nm and (b) the corresponding spectra of PtL^{1}SR complexes.

complexes are weaker emitters than their benzenethiolate analogues, with lower quantum yields and shorter lifetimes.

(vi) All spectra are strongly blue-shifted in a glass at 77 K in comparison to the spectra at room temperature (Table 2; spectra for PtL^{2}SAr series are shown in Figure 6 and for PtL^{1}SAr in Figure S3 (Supporting Information)). The temperature-induced shifts are largest for the two nitro-substituted

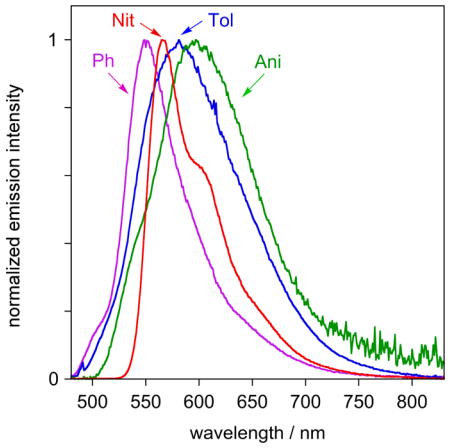

Figure 6. Emission spectra of PtL^{2}SR complexes at 77 K in EPA, λ_{ex} = 460 nm (EPA = diethyl ether/isopentane/ethanol, 2:2:1 v/v).

complexes (3400 cm^{-1}), most of the others having values of around 2500 cm^{-1}. The lifetimes of the nitro-substituted complexes at 77 K are conspicuously very long, around 2 orders of magnitude longer than those of the other complexes.

Assuming that the excited state is formed with unitary efficiency, we can estimate the radiative, k_r, and nonradiative, $\sum k_{nr}$, decay rate constants from the experimentally determined quantum yields and lifetimes: $k_r = \Phi/\tau$ and $\sum k_{nr} = \tau^{-1} - k_r$. The data (Table 2) reveal that the radiative rate constants for the nitro complexes are 2−3 orders of magnitude smaller than for the other arenethiolate and methanethiolate complexes.

Time-Dependent Density Functional Theory (TD-DFT) and Interpretation of Emission Data. These observations can be rationalized successfully with the aid of time-dependent density functional theory (TD-DFT) calculations, to evaluate the nature of the lowest-energy triplet state, T_1, from which emission occurs. The triplet state geometry was first optimized by direct calculation (i.e., by minimization of the geometry with a triplet spin), and then frequency calculations were utilized to confirm that the geometries obtained were true minima. TD-DFT calculations were performed on the optimized geometries to give the frontier orbitals and the relative contributions of transitions between filled and virtual orbitals to the lowest

Table 2. Luminescence Data for the Platinum Complexes in CH_2Cl_2 Solution at 298 K and in EPA[a] at 77 K

						emission 77 K		
complex	emission λ_{max}/nm	$\Phi_{lum} \times 10^{2b}$	τ/ns	$k_r/10^3$ s^{-1c}	$\sum k_{nr}/10^4$ s^{-1c}	λ_{max}/nm	$\Delta E^{77K-298\ K}$/cm^{-1d}	τ/ns
PtL^{1}Cl	*491, 524, 562*	60	7200	83	5.5	*486, 516, 548*	210	6400
PtL^{1}SMe	636	2.6	430	60	230	538	2860	6600
PtL^{1}SPh	634	17	770	220	110	539	2780	6800
PtL^{1}STol	661	6.9	510	140	180	548	3120	7400
PtL^{1}SAni	691	1.4	48	290	2100	570	3070	8200
PtL^{1}SNit	714	0.21	7400	0.28	13	574, 610	3420	7.6×10^5
PtL^{2}Cl	*481, 513, 550*	58	8000	72	5.3	*478, 510, 547*	130	7000
PtL^{2}SMe	642	3.8	510	75	190	558	2340	6600
PtL^{2}SPh	643	16	880	180	95	550	2630	7800
PtL^{2}STol	668	6.0	370	160	250	581	2240	8900
PtL^{2}SAni	701	0.35	29	120	3400	597	2490	9500
PtL^{2}SNit	703	0.64	11300	0.57	8.8	567, 603	3410	4.7×10^5

[a]EPA = diethyl ether/isopentane/ethanol, 2/2/1 v/v. [b]Measured using $[Ru(bpy)_3]Cl_2$ as the standard. [c]k_r and $\sum k_{nr}$ are the radiative and nonradiative rate constants estimated from the quantum yield and lifetime at 298 K. [d]Difference in energy of emission at 77 K in comparison to 298 K estimated using the λ_{max} values.

dx.doi.org/10.1021/ic500555w | Inorg. Chem. 2014, 53, 5738−5749

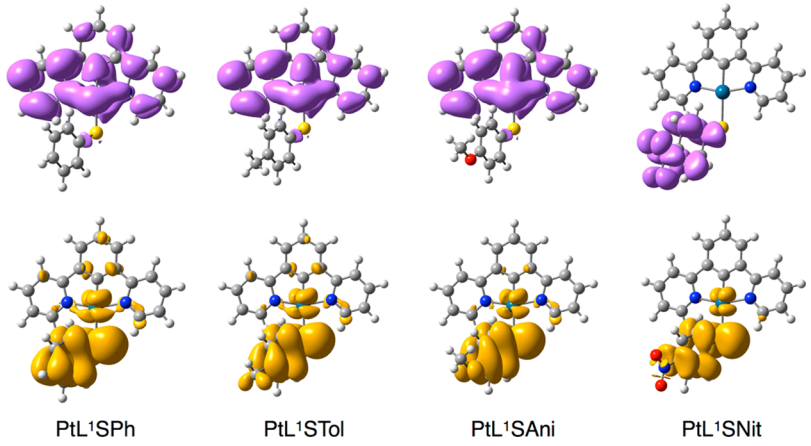

Figure 7. Density difference plots for the triplet states of PtL¹SAr, obtained by TD-DFT using PBE0 and the PCM model for dichloromethane as the solvent. Purple and yellow represent zones of augmentation and depletion of electron density, respectively, in the excited state relative to the ground state.

triplet excited states. Frontier orbitals and tables of contributions for the PtL¹SR series of complexes are shown in Figure S4 and Table S2 in the Supporting Information. The corresponding density difference plots—which take into account all of the contributions and hence provide a more informative picture of the rearrangement of electron density in the exctied state—are shown in Figure 7. They show that the excited state has $d_{Pt}/\pi_{RS} \rightarrow \pi^*_{NCN}$ character for the phenyl, tolyl, and anisyl complexes.

A directional charge-transfer excited state of this type readily accounts for several of the experimental trends in emission data for the complexes with these substituents listed above. (i) The lower energy of each PtL²SR complex in comparison to its PtL¹SR analogue (except R = Nit; see below) can be rationalized in terms of the electron-withdrawing ester group stabilizing the NCN-based LUMO. The effect is, however, rather small, since the ester lies in the central aryl group rather than the pyridyl rings which dominate the LUMO. (ii) The trend of decreasing emission energy in the order SPh > STol > SAni is consistent with the increasing electron-donating power of the substituent, which will favor charge transfer from the thiolate. The gradient of 7800 cm^{-1}/V from the plot of E_{em} versus $|E^{ox} - E^{red}|$ mentioned above is quite large, suggesting a significant charge-transfer character. Indeed, the value is remarkably similar to that of 7300 cm^{-1}/V found for a selection of 13 complexes of the form Pt(N^N)(S^S) studied by Cummings and Eisenberg.[26d] In that case too, all the evidence pointed toward a charge-transfer-to-diimine assignment to the lowest-energy singlet and triplet excited states. Finally, observation vi, namely the large blue shift of the emission maxima observed on cooling to 77 K, is consistent with an excited state in which there is a high degree of charge transfer in a well-defined direction. The substantial rearrangement of electron density that is associated with the formation of such an excited state is accompanied by significant solvent reorganization to stabilize the excited state (large Stokes shift). Such stabilization is inhibited in a frozen glass, leading to a large temperature-induced shift, as observed here. The contrast with PtL¹Cl and PtL²Cl is particularly dramatic in this respect: they show only very small shifts on cooling to 77 K (Table 2), consistent with the largely N^C^N-based $^3\pi-\pi^*$ assignment of the excited state in these parent chloro complexes.[23]

A point to consider in excited states with heavily mixed contributions of metal and ligand, as in this case of $d_{Pt}/\pi_{RS} \rightarrow \pi^*_{NCN}$, is the relative contribution of the metal and ligand: i.e., the Pt and RS^- units. In other words, is assignment as MLCT or LLCT more appropriate? The Mulliken charges on the metal and the two different ligands in each of the PtL¹SAr complexes are given in Table S3 of the Supporting Information. They provide a crude, albeit convenient, means of quantifying the relative importance of metal and thiolate orbitals. It can be seen that the relative contribution of the thiolate increases, and that of the metal decreases, on going from phenyl through tolyl to anisyl. One could thus describe a trend toward increasing LLCT character at the expense of MLCT character as the electron-donating power of the thiolate increases.

The TD-DFT results for the nitro-substituted complex give a strikingly different picture; in this case, the excited state is seen to be localized on the arenethiolate, with essentially no involvement of either the metal or the N^C^N ligand. The most fitting description is that of a $\pi(SC_6H_4) \rightarrow \pi^*(NO_2)$ transition, in line with that observed in the previously reported complexes of this ligand mentioned above.[27a,30] The Mulliken charges are again useful, in this case in highlighting the lack of involvement of the N^C^N ligand.

The differing nature of the excited state in PtL″SNit accounts for the observed differences in the photoluminescence properties for the nitro complexes in comparison to the others listed above. The deviation from the E_{em} versus $|E^{ox} - E^{red}|$ plot (Figure 4, bottom) is accounted for. The slightly higher energy of the emission of PtL²SNit compared to PtL¹SNit can be explained by a small influence of the ester in stabilizing the Pt/S filled orbitals (HOMO), but with no effect on the nitrophenyl-based LUMO. Moreover, the much longer luminescence lifetimes observed for the nitro complexes (both at room temperature and at 77 K) can be explained, in part, by the more limited participation of the metal in the excited state. Significant involvement of the metal is required to successfully promote the formally forbidden $T_1 \rightarrow S_0$ radiative transition,[31] whereas the TD-DFT (Figure 7) indicates an essentially ligand-centered (ILCT) transition. As a result, the k_r values for these two complexes are much lower than for all the others.

It is notable, however, that this complex seems to "fit" well with the E_{abs} versus $|E^{ox} - E^{red}|$ plot (Figure 4, top). Indeed, in UV−Visible Absorption Spectra, we interpreted the absorption spectrum in terms of a lowest-energy transition to a singlet excited state having the same charge transfer to N^C^N

dx.doi.org/10.1021/ic500555w | Inorg. Chem. 2014, 53, 5738−5749

character as that of the other complexes, superimposed on a more intense but higher-energy transition more localized on the nitrobenzenethiolate ligand. Such a difference between absorption and emission (i.e., differing orbital parentage of the S_1 and T_1 excited states) is quite plausible. Excited states with a high degree of charge transfer have smaller S−T energy gaps than those which are more localized, and hence $^3[d_{Pt}/\pi_{RS} \rightarrow \pi^*_{NCN}]$ may be higher in energy than $^3[\pi(SC_6H_4) \rightarrow \pi^*(NO_2)]$ even though $^1[d_{Pt}/\pi_{RS} \rightarrow \pi^*_{NCN}]$ is lower in energy than $^1[\pi(SC_6H_4) \rightarrow \pi^*(NO_2)]$.

Nonradiative Decay Trends. It is instructive to inspect in more detail the nonradiative decay rate constants. Typically, for compounds with a mutually common type of excited state, the nonradiative decay constant should increase as the excited state energy decreases, owing to the increased probability of intramolecular energy transfer into high-energy vibrational modes within the molecule. Detailed quantitative treatments indicate that a logarithmic dependence may be anticipated,[14] as observed in some classic studies with ruthenium and with platinum complexes, for example.[15−17] Figure 8 illustrates a plot

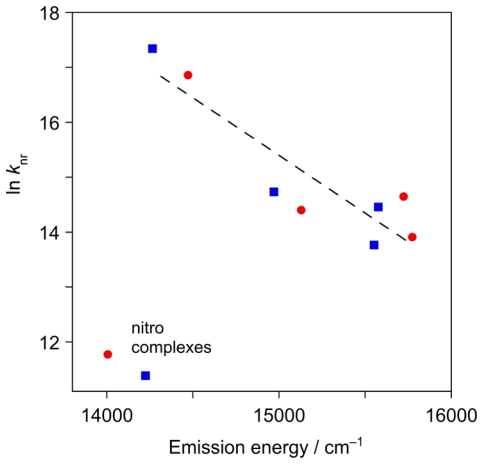

Figure 8. Plot of ln k_{nr} versus the emission energy. The complexes of L^1 are represented by red circles and those of L^2 by blue squares. The dashed black line is the least-squares linear fit through all data points except for the two nitro-substituted complexes (which appear in the bottom left of the graph).

of {ln k_{nr}} versus the excited state energy, estimated from the emission maxima,[32] for the eight aryl-substituted complexes. It can be seen that there is a convincing linear relationship, but only if the nitro-substituted compounds are excluded. They are seen to have much lower nonradiative decay constants than would be anticipated for their emission energies, if they had excited states similar to those of the other aryl-substituted complexes. Clearly, this observation provides further evidence in support of a very different nature of the excited state in these two complexes.

Intermolecular Interactions. The parent complex PtL^1Cl is known to display a quite sensitive dependence of the emission spectrum upon concentration. The lifetime decreases with concentration at values greater than around 10^{-5} M, accompanied by the appearance of an excimer emission band centered at about 700 nm.[8] Derivatives incorporating substituents in the tridentate ring behave similarly, albeit typically with smaller Stern−Volmer quenching constants and, in some cases, significantly shifted excimer bands.[12] For the present set of complexes, there was no significant self-quenching observed in solution at room temperature over a 20-fold concentration range (up to 4×10^{-4} M), nor was there was any evidence for excimer emission.[33] The lack of effect could be associated with the greater steric hindrance engendered by the arenethiolate to the face-to-face approach of pairs of molecules, which is necessary for excimers to form (the optimum distance is typically around 3.5 Å). It should also be noted that the excited state lifetime in the thiolate complexes is 1 order of magnitude shorter than in PtL^1Cl, and the propensity to excimer formation will necessarily decrease for that reason as well. Steric hindrance to interfacial interactions should be minimal in the case of the methanethiolate complexes, but again, no significant concentration-induced quenching was observed. However, for this pair of complexes it was noted that, at 77 K, elevated concentrations led to the appearance of an additional low-energy emission band (Figure S5). The excitation spectra registered for the two emission bands are slightly different from one another around the low-energy tail, suggesting that the additional band may be due to the formation of a ground-state aggregate. No such behavior was observed for the arenethiolate complexes.

Relevance to Biological Thiols and Bioimaging Applications. PtL^1Cl and its derivatives have been investigated as cell imaging agents.[4a,e] The studies to date reveal that they localize in the nuclei of a variety of cell lines, from which intense green emission with the characteristic spectrum of the Pt(N^C^N) unit is observed, with a lifetime of around 1 μs. The fate of the rather labile Pt−Cl bond is, however, rather uncertain, and it is possible that the observed nuclear localization is due to platination of nucleobases or histidine residues through their nitrogen atoms. In the event that the Pt−Cl bond is displaced by a thiolate group of a cysteine residue within a protein, however, green emission might no longer be expected, but rather a shift to red emission, on the basis of the results described in Photoluminescence and illustrated in Figure 2.

In order to explore this possibility, NIH 3T3 cells incubated with PtL^1Cl were imaged using fluorescence microscopy in two different regions of the spectrum. When the emission was monitored in the green region, the typical nuclear staining seen previously[4a] was observed (Figure 9a). However, when the emission was monitored using a longer-wavelength emission filter (660−710 nm) that completely eliminates green light but transmits only red light, a distinctly different localization pattern was revealed (Figure 9b). Emission in that case was observed mainly within the cytoplasmic region. The cytoplasmic emission is not homogeneous in the image: emission emanates from discrete areas within a cytoplasm-based organelle. Costaining of CHO cells with PtL^1Cl and MitoTracker Red (MTR) suggests that the organelles in question are the mitochondria (Figure S6 (Supporting Information)).

It is notable that the mitochondria typically contain an abundance of thiols.[34] Indeed, recent work indicates that the labeling of protein targets by MTR involves covalent bond formation and is related to the availability of cysteine residues.[35] Meanwhile, Coogan and co-workers have developed rhenium complexes to stain mitochondria in which protein thiols react with a 3-chloromethylpyridyl group on the complex.[36] Thus, it seems likely that the emission detected in Figure 9b is due to thiolate adducts of the form PtL^1SR. We note that Chan and co-workers have observed a diminution of the green luminescence from Pt(N^C^N)Cl units upon treatment with

dx.doi.org/10.1021/ic500555w | Inorg. Chem. 2014, 53, 5738−5749

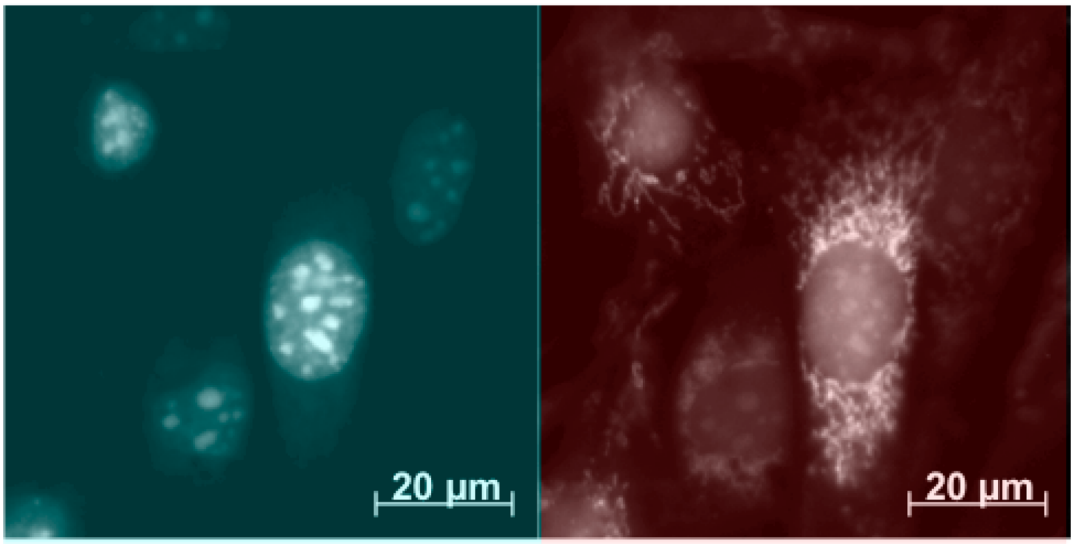

Figure 9. Fluorescence microscopy images of NIH 3T3 cells incubated with PtL^1Cl (50 μM, 5 min): (left) image acquired using a G365ex/FITCem filter set (green emission region only); (right) image acquired using a G365ex/660−710em filter set (red emission only).

cysteine, interpreted in terms of displacement of the chloride ligand by a cysteine sulfur atom.[37] In their case, no red emission appeared, but this may be due to efficient quenching of the emission under the polar aqueous conditions employed.

Concluding Discussion. PtL^1Cl and derivatives featuring modified tridentate ligands have emerged over the past decade as a family of complexes that offer unusually high phosphorescence quantum yields. However, the emission is typically limited to the green or yellow region, and the replacement of the chloride ligand by other anionic and neutral ligands, such as phenolates and pyridine derivatives, respectively, has little effect, since the excited state is based primarily on the Pt(N^C^N) unit. The present work has revealed that the use of electron-rich thiolates as monodentate coligands leads to a profound change in the nature of the lowest-energy singlet and triplet excited states, to ones which feature charge transfer from the thiolate (mixed with some metal character) to the tridentate ligand. This leads to a red shift in the absorption and phosphorescence. Although the luminesence quantum yields are reduced in comparison to those of the parent complexes, the values of around 0.16 for the benzenethiolate complexes are unusually high for platinum(II) complexes that emit at such low energy, deep into the red region of the spectrum. The ability to further tune the properties of this interesting class of complex may open up new potential, for example, in the fields of solar energy conversion and bioimaging, where lower-energy absorption and emission, respectively, are important. Although the stability of the complexes in solution is rather low, it may be noted that the previously reported instability of the corresponding phenolate complexes has been successfully overcome by covalent linkage of the phenolate to the N^C^N unit, to generate a tetradentate ligand.[38] A similar strategy involving arenethiolates looks set to offer a promising approach to stable, red-emitting platinum(II) complexes.

■ EXPERIMENTAL SECTION

The complexes PtL^1Cl and PtL^2Cl were prepared as described previously.[39,8] ^1H and ^{13}C NMR spectra, including NOESY and COSY, were recorded on Varian or Bruker spectrometers operating at the frequencies indicated below. It was possible to obtain ^{13}C spectra with full assignment only in the cases indicated. For the other complexes (for which either the solubility is lower or the stability inferior), impurities begin to form during the time necessary to acquire the ^{13}C spectrum, hampering the assignment. Chemical shifts (δ) are in ppm, referenced to residual protio-solvent resonances, and coupling constants are in hertz. Electron ionization mass spectra were acquired at the EPSRC National Mass Spectrometry Service Centre, Swansea, U.K., using perfluorotributylamine as the standard for accurate mass measurements. All solvents used in preparative work were at least Analar grade, and water was purified using the Purite system. Solvents used for optical spectroscopy were HPLC grade. In all but three cases, elemental analyses gave percent C, H, N data to within the normally accepted limit of 0.4% of the theoretical values. The exceptions were PtL^1SNit and the complexes of methanethiolate, PtL^1SMe and PtL^2SMe, where percent C deviations were slightly larger. Repeated attempts to obtain improved quality samples failed to give better data, mostly likely due to traces of the decomposition product forming in solution, as discussed in Synthesis of Complexes.

PtL^1SMe. Sodium methanethiolate (50 mg, 0.15 mmol, 21% w/w in H_2O) was dissolved in methanol (5 mL) and the solution degassed via four freeze−pump−thaw cycles prior to back-filling the reaction vessel with nitrogen gas. PtL^1Cl (63 mg, 0.14 mmol) was added under a flow of nitrogen, and the suspension was stirred at room temperature for 18 h. The solid was separated using a centrifuge, washed successively with methanol (5 mL), water (3 × 5 mL), and diethyl ether (2 × 5 mL), and finally dried under reduced pressure, giving the desired product as an orange solid (26 mg, 40%). ^1H NMR (400 MHz, d_6-DMSO): δ 9.40 (2H, d, ^3J = 4.8, $^3J(^{195}Pt)$ = 42, H^6), 8.19 (2H, t, ^3J = 8.0, H^4), 8.11 (2H, d, ^3J = 6.4, H^3), 7.81 (2H, d, ^3J = 7.6, $H^{3'}$), 7.53 (2H, t, ^3J = 6.4, H^5), 7.29 (1H, t, ^3J = 7.6, $H^{4'}$), 2.23 (3H, s, CH_3). ^{13}C NMR (125.7 MHz, d_6-DMSO): δ 167.9, 152.2, 140.9, 140.2, 124.8, 124.1, 123.4, 120.5, 12.6. Anal. Calcd for $C_{17}H_{14}N_2PtS$: C, 43.13; H, 2.98; N, 5.92%. Found: C, 42.57; H, 2.90; N, 5.75%.

PtL^1SPh. Thiophenol (47 mg, 0.42 mmol) was dissolved in methanol (6 mL) and the solution degassed via four freeze−pump−thaw cycles before being placed under an atmosphere of nitrogen. Potassium *tert*-butoxide (48 mg, 0.43 mmol) was added under a flow of nitrogen gas, and the mixture was stirred for 5 min followed by addition of PtL^1Cl (129 mg, 0.28 mmol). The suspension was stirred at room temperature for 16 h under nitrogen. The solid was then separated by centrifugation, washed successively with methanol and diethyl ether (3 × 5 mL of each), and dried under vacuum, to give the product as a yellow solid (120 mg, 80%). ^1H NMR (500 MHz, d_6-DMSO): δ 9.19 (2H, d, ^3J = 5.5, $^3J(^{195}Pt)$ = 38, H^6), 8.14 (4H, overlapping m, H^3 and H^4), 7.81 (2H, d, ^3J = 7.5, $H^{3'}$), 7.51 (2H, d, ^3J

dx.doi.org/10.1021/ic500555w | Inorg. Chem. 2014, 53, 5738−5749

= 7.5, $H^{2''}$), 7.40 (2H, m, H^5), 7.31 (1H, t, ^3J = 7.5, $H^{4'}$), 6.94 (2H, t, ^3J = 7.5, $H^{3''}$), 6.79 (1H, t, ^3J = 7.5, $H^{4''}$). ^{13}C NMR (HSQC observe ^{1}H 500 MHz, decouple ^{13}C 125.7 MHz and HMBC observe ^{1}H 500 MHz, d_6-DMSO): δ 169.1 ($C^{1'}$), 167.8 (C^2), 152.7 (C^6), 148.8 ($C^{1''}$), 141.2 ($C^{2'}$), 140.3 (C^4), 132.2 ($C^{2''}$), 127.6 ($C^{3''}$), 124.8 ($C^{3'}$), 124.1 (C^5), 123.8 ($C^{4'}$), 121.1 ($C^{4''}$), 120.5 (C^3). MS (EI): m/z 535 M^+, 426 $[M - SPh]^+$. HRMS (EI): m/z 535.0675, calcd for $C_{22}H_{16}N_2SPt$ m/z 535.0676. Anal. Calcd for $C_{22}H_{16}N_2PtS$: C, 49.34; H, 3.01; N, 5.23. Found: C, 48.96; H, 2.95; N, 5.14.

PtL^{1}STol. This complex was prepared in a manner similar to that for PtL^{1}SPh, starting from PtL^{1}Cl (128 mg, 0.28 mmol), 4-methylthiophenol (55 mg, 0.44 mmol), and KO^{t}Bu (60 mg, 0.54 mmol), leading to the product as an orange solid (118 mg, 78%). ^{1}H NMR (500 MHz, d_6-DMSO): δ 9.19 (2H, d, ^3J = 5.5, $^3J(^{195}Pt)$ = 30, H^6), 8.14 (4H, m, H^3 and H^4), 7.82 (2H, d, ^3J = 8.0, $H^{3'}$), 7.41 (2H, t, ^3J = 7.5, H^5), 7.39 (2H, d, ^3J = 8.0, $H^{2''}$), 7.32 (1H, t, ^3J = 8.0, $H^{4'}$), 6.77 (2H, d, ^3J = 8.0, $H^{3''}$) 2.12 (3H, s, CH_3). ^{13}C NMR (HSQC observe ^{1}H 500 MHz, decouple ^{13}C 125.7 MHz and HMBC observe ^{1}H 500 MHz, d_6-DMSO): δ 170.0 ($C^{1'}$), 168.5 (C^2), 153.3 (C^6), 145.4 ($C^{1''}$), 141.8 ($C^{2'}$), 141.0 (C^3), 132.8 ($C^{2''}$), 130.5 ($C^{4''}$), 129.1 ($C^{3''}$), 125.5 ($C^{3'}$), 124.8 (C^5), 124.4 ($C^{4'}$), 121.2 (C^4), 20.44 (CH_3). Anal. Calcd for $C_{23}H_{18}N_2PtS$: C, 50.27; H, 3.30; N, 5.10. Found: C, 49.89; H, 3.19; N, 4.92.

PtL^{1}SAni. This complex was prepared in a manner similar to that for PtL^{1}SPh, starting from PtL^{1}Cl (30 mg, 0.065 mmol), 4-methoxythiophenol (23 mg, 0.16 mmol), and KO^{t}Bu (21 mg, 0.19 mmol), giving the product as a red solid (20 mg, 55%). ^{1}H NMR (400 MHz, d_6-DMSO): δ 9.18 (2H, d, ^3J = 4.8, $^3J(^{195}Pt)$ = 18, H^6), 8.13 (4H, m, H^3 and H^4), 7.82 (2H, d, ^3J = 7.5, $H^{3'}$), 7.40 (2H, m, H^5), 7.39 (2H, d, ^3J = 8.5, $H^{2''}$), 7.32 (1H, t, ^3J = 7.5, $H^{4'}$), 6.59 (2H, d, ^3J = 8.5, $H^{3''}$), 3.61 (3H, s, OCH_3). ^{13}C NMR (HSQC, observe ^{1}H 500 MHz, decouple ^{13}C 125.7 MHz, d_6-DMSO): δ 167.9 (quat), 152.5 (C^6), 141.1 (quat), 140.3 (C^3 or C^4), 133.1 (C^5 or $C^{2''}$ or $C^{3''}$), 124.8 ($C^{3'}$), 124.0 (C^5 or $C^{2''}$ or $C^{3''}$), 123.6 ($C^{4'}$), 120.5 (C^3 or C^4), 113.6 ($C^{2''}$ or $C^{3''}$), 54.9 (OCH_3); remaining quaternaries were not detected. Anal. Calcd for $C_{23}H_{18}N_2OPtS$: C, 48.85; H, 3.21; N, 4.95. Found: C, 48.54; H, 3.16; N, 4.92.

PtL^{1}SNit. This compound was prepared from PtL^{1}Cl (52 mg, 0.13 mmol), 4-nitrothiophenol (36 mg, 0.23 mmol), and KO^{t}Bu (25 mg, 0.23 mmol), using the same procedure as for PtL^{1}SPh, giving the product as a red-orange solid (52 mg, 72%). ^{1}H NMR (400 MHz, d_6-DMSO): δ 9.08 (2H, d, ^3J = 6.0, $^3J(^{195}Pt)$ 30, H^6) 8.17 (4H, m, H^3 and H^4), 7.84 (2H, d, ^3J = 7.5, $H^{3'}$), 7.82 (2H, d, ^3J = 8.5, $H^{2''}$ or $H^{3''}$), 7.71 (2H, d, ^3J = 8.5, $H^{2''}$ or $H^{3''}$), 7.46 (2H, t, ^3J = 6.5, H^5), 7.35 (1H, t, ^3J = 7.5, $H^{4'}$). MS (EI): m/z 581 M^+, 426 $[M - SC_6H_4NO_2]^+$. HRMS (EI): m/z 580.0529, calcd for $C_{22}H_{15}N_3O_2SPt$ m/z 580.0527. Anal. Calcd for $C_{22}H_{15}N_3O_2PtS$: C, 45.52; H, 2.60; N, 7.24. Found: C, 44.57; H, 2.58; N, 6.51.

PtL^{2}SMe. This complex was prepared using the method described for PtL^{1}SMe, starting from PtL^{2}Cl (45.8 mg, 0.088 mmol) and sodium methanethiolate (31 mg, 0.092 mmol, 21% w/w in H_2O) in methanol (5 mL), leading to the product as an orange-red solid (24 mg, 51%). ^{1}H NMR (400 MHz, d_6-DMSO): δ 9.39 (2H, d, ^3J = 5.0, $^3J(^{195}Pt)$ = 42, H^6), 8.73 (2H, d, ^3J = 7.0, H^3), 8.33 (2H, s, $H^{3'}$), 8.21 (2H, t, ^3J = 7.5, H^4), 7.58 (2H, t, ^3J = 7.0, H^5), 3.90 (3H, s, OCH_3), 2.26 (3H, s, SCH_3). Anal. Calcd for $C_{19}H_{16}N_2O_2PtS$: C, 42.94; H, 3.03; N, 5.27. Found: C, 42.50; H, 2.98; N, 4.92.

PtL^{2}SPh. The title compound was prepared using the same procedure as that described for PtL^{1}SPh, starting from PtL^{2}Cl (93 mg, 0.18 mmol), thiophenol (41 mg, 0.37 mmol), and KO^{t}Bu (46 mg, 0.41 mmol), leading to the product as a yellow solid (86 mg, 81%). ^{1}H NMR (400 MHz, d_6-DMSO): δ 9.19 (2H, d, ^3J = 5.0, $^3J(^{195}Pt)$ = 38, H^6), 8.35 (2H, s, $H^{3'}$), 8.29 (2H, d, ^3J = 8.0, H^3), 8.18 (2H, t, ^3J = 7.5, H^4), 7.51 (2H, d, ^3J = 7.5, $H^{2''}$), 7.45 (2H, t, ^3J = 7.0, H^5), 6.97 (2H, t, ^3J = 7.5, $H^{3''}$), 6.82 (1H, t, ^3J = 7.5, $H^{4''}$), 3.92 (3H, s, OCH_3). MS (EI): m/z 593 (M^+), 484 (M^+ − thiolate), 425 (M^+ − thiolate − CO_2Me), 110 (thiol$^+$). HRMS (EI): m/z 593.0726 (M^+), calcd for $C_{24}H_{18}N_2O_2PtS$ 593.0731. Anal. Calcd for $C_{24}H_{18}N_2O_2PtS$: C, 48.56; H, 3.06; N, 4.72. Found: C, 48.34; H, 3.03; N, 4.59.

PtL^{2}STol. This complex was prepared similarly, from PtL^{2}Cl (98 mg, 0.19 mmol), 4-methylthiophenol (50 mg, 0.40 mmol), and KO^{t}Bu (50 mg, 0.045 mmol), leading to the product as a yellow-orange solid (78 mg, 68%). ^{1}H NMR (400 MHz, d_6-DMSO): δ 9.22 (2H, d, ^3J = 4.0, $^3J(^{195}Pt)$ = 28, H^6), 8.40 (2H, s, $H^{3'}$), 8.32 (2H, d, ^3J = 8.5, H^3), 8.20 (2H, t, ^3J = 8.5, H^4), 7.48 (2H, t, ^3J = 6.0, H^5), 7.38 (2H, d, ^3J = 8.5, $H^{2''}$), 6.79 (2H, d, ^3J = 8.5, $H^{3''}$), 3.92 (3H, s, OCH_3), 2.13 (3H, s, CH_3). MS (EI): m/z 607 (M^+), 484 (M^+ − thiolate), 425 (M^+ − thiolate − CO_2Me), 124 (thiol$^+$), 91 ($C_7H_7^+$). HRMS (EI): m/z 607.0889 (M^+), calcd for $C_{25}H_{20}N_2O_2PtS$ 607.0888. Anal. Calcd for $C_{25}H_{20}N_2O_2PtS$: C, 49.42; H, 3.32; N, 4.61. Found: C, 49.20; H, 3.29; N, 4.42.

PtL^{2}SAni. The title complex was prepared in the same way, starting from PtL^{2}Cl (50 mg, 0.096 mmol), 4-methoxythiophenol (28 mg, 0.20 mmol), and KO^{t}Bu (24 mg, 0.21 mmol), leading to the product as a red solid (43 mg, 71%). ^{1}H NMR (400 MHz, d_6-DMSO): δ 9.19 (2H, d, ^3J = 5.6, $^3J(^{195}Pt)$ = 38, H^6), 8.38 (2H, s, $H^{3'}$), 8.31 (2H, d, ^3J = 8.4, H^3), 8.19 (2H, t, ^3J = 7.2, H^4), 7.47 (2H, t, ^3J = 6.8, H^5), 7.38 (2H, d, ^3J = 8.4, $H^{2''}$), 6.61 (2H, d, ^3J = 8.4, $H^{3''}$), 3.92 (3H, s, $COOCH_3$), 3.62 (3H, s, OCH_3). Anal. Calcd for $C_{25}H_{20}N_2O_3PtS$: C, 48.15; H, 3.32; N, 4.49. Found: C, 48.01; H, 3.17; N, 4.46.

PtL^{2}SNit. This complex was also prepared using the same general procedure, from PtL^{2}Cl (96 mg, 0.19 mmol), 4-nitrothiophenol (59 mg, 0.38 mmol), and KO^{t}Bu (44 mg, 0.39 mmol), giving the product as a yellow solid (109 mg, 92%). ^{1}H NMR (300 MHz, d_6-DMSO): δ 9.03 (2H d, ^3J = 5.0, $^3J(^{195}Pt)$ = 34, H^6), 8.91 (4H, m, H^3 and H^4), 8.26 (2H, s, $H^{3'}$), 7.80 (2H, d, ^3J = 8.0, $H^{2''}$ or $H^{3''}$), 7.66 (2H, d, ^3J = 8.0, $H^{3''}$ or $H^{2''}$) 7.47 (2H, t, ^3J = 5.5, H^5), 3.92 (3H, s, OCH_3). MS (EI): m/z 640 (M^+), 484 (M^+ − thiolate), 425 (M^+ − thiolate − CO_2Me), 155 (thiol$^+$). HRMS (EI): m/z 638.0579 (M^+), calcd for $C_{24}H_{17}N_3O_4PtS$ 638.0582. Anal. Calcd for $C_{24}H_{17}N_3O_4PtS$: C, 45.14; H, 2.63; N, 6.58. Found: C, 44.96; H, 2.67; N, 6.43.

Electrochemistry. Cyclic voltammetry was carried out using a μAutolab Type III potentiostat with computer control and data storage via GPES Manager software. Solutions of concentration ca. 1 mM in CH_2Cl_2 were used, containing $[Bu_4N][PF_6]$ as the supporting inert electrolyte. A three-electrode assembly was employed, consisting of a glassy-carbon working electrode and platinum-wire counter and reference electrodes. Solutions were purged for 5 min with solvent-saturated nitrogen gas with stirring, prior to measurements being taken without stirring. The voltammograms were referenced to the ferrocenelferrocenium couple ($E_{1/2}$ = 0.42 V versus SCE).

Density Functional Theory Calculations. The Gaussian 09 program was used for all calculations.[40] DFT calculations for geometries and excitation energies were performed with the PBE0 hybrid exchange-correlation functional.[41,42] The all-electron cc-pVDZ basis set was used on the main-group atoms. For the platinum ion, the Los Alamos LANL2DZ effective core potentials were used to treat the core electrons, in combination with the LANL2DZ basis set for the $5s^2$, $5p^6$, and $5d^8$ valence electrons. The geometries were fully optimized without symmetry constraints. The polarizable continuum model (PCM) was used to take into account the solvent (dichloromethane). Frequency calculations were performed at the same level of theory as the geometry optimizations to ensure that the identified geometries do indeed correspond to minima on the potential energy surface. Density difference plots were produced with Gaussview using the default contour value of 0.02 au.

Photophysical Measurements. Absorption spectra were measured on a Biotek Instruments XS spectrometer, using quartz cuvettes of 1 cm path length. Steady-state luminescence spectra were measured using a Jobin Yvon FluoroMax-2 spectrofluorimeter, fitted with a red-sensitive Hamamatsu R928 photomultiplier tube; the spectra shown are corrected for the wavelength dependence of the detector, and the quoted emission maxima refer to the values after correction. Samples for emission measurements were contained within quartz cuvettes of 1 cm path length modified with appropriate glassware to allow connection to a high-vacuum line. Degassing was achieved via a minimum of three freeze−pump−thaw cycles while the cuvette was connected to the vacuum manifold; the final vapor pressure at 77 K was $<5 \times 10^{-2}$ mbar, as monitored using a Pirani gauge. Luminescence

dx.doi.org/10.1021/ic500555w | Inorg. Chem. 2014, 53, 5738−5749

quantum yields were determined using $[Ru(bpy)_3]Cl_2$ in degassed aqueous solution as the standard (ϕ = 0.042[43]); the estimated uncertainty in Φ is ±20% or better.

The luminescence lifetimes of the complexes were measured by time-correlated single-photon counting, following excitation at 374.0 nm with an EPL-375 pulsed-diode laser. The emitted light was detected at 90° using a Peltier-cooled R928 PMT after passage through a monochromator. The estimated uncertainty in the quoted lifetimes is ±10% or better. Lifetimes at 77 K in excess of 10 μs were measured by multichannel scaling following excitation with a microsecond-pulsed xenon lamp; an excitation wavelength of 374 nm (band pass 5 nm) was selected with a monochromator.

Cell Imaging. The instrumentation and procedures for imaging of NIH 3T3 or CHO cells incubated with the complex were as described in previous work.[4a,44]

■ ASSOCIATED CONTENT

Ⓢ Supporting Information

Figures and tables giving absorption spectra and λ_{max} values of the complexes in a selection of different solvents, emission spectra of the PtL^1SR complexes at 77 K, emission spectrum of a concentrated solution of PtL^2SMe at 77 K, fluorescence microscopy images of CHO cells costained with PtL^1Cl and MitoTracker Red, and further TD DFT data, including frontier orbital plots and Mulliken charges. This material is available free of charge via the Internet at http://pubs.acs.org.

■ AUTHOR INFORMATION

Corresponding Author

*E-mail for J.A.G.W.: j.a.g.williams@durham.ac.uk.

Notes

The authors declare no competing financial interest.

■ ACKNOWLEDGMENTS

We thank the EPSRC (studentship to G.R.F., grant ref EP/G06928X/1), ONE North East, and Durham University (studentship for W.A.T.). We thank the EPSRC National Mass Spectrometry Service Centre, Swansea, U.K., for recording EI mass spectra.

■ REFERENCES

(1) (a) Xiang, H.-F.; Lai, S.-W.; Lai, P. T.; Che, C.-M. Phosphorescent platinum(II) materials for OLED applications. In *Highly efficient OLEDs with phosphorescent materials*; Yersin, H., Ed.; Wiley-VCH: Weinheim, Germany, 2008. (b) Williams, J. A. G.; Develay, S.; Rochester, D. L.; Murphy, L. *Coord. Chem. Rev.* **2008**, *252*, 2596. (c) Chi, Y.; Chou, P. T. *Chem. Soc. Rev.* **2010**, *39*, 638. (d) Kalinowski, J.; Fattori, V.; Cocchi, M.; Williams, J. A. G. *Coord. Chem. Rev.* **2011**, *255*, 2401. (e) Gildea, L. F.; Williams, J. A. G. Iridium and platinum complexes for OLEDs. In *Organic light-emitting diodes: Materials, devices and applications*; Buckley, A., Ed.; Woodhead: Cambridge, U.K., 2013.

(2) (a) Fletcher, N.; Lagunas, M. C. *Top. Organomet. Chem.* **2010**, *28*, 143. (b) Tang, W.-S.; Lu, X.-X.; Wong, K. M.-C.; Yam, V. W.-W. *J. Mater. Chem.* **2005**, *15*, 2714. (c) Siu, P. K. M.; Lai, S.-W.; Lu, W.; Zhu, N.; Che, C.-M. *Eur. J. Inorg. Chem.* **2003**, 2749. (d) Yang, Q.-Z.; Tong, Q.-X.; Wu, L.-Z.; Zhang, L.-P.; Tung, C.-H. *Eur. J. Inorg. Chem.* **2004**, 1948. (e) Lanoë, P.-H.; Fillaut, J.-L.; Toupet, L.; Williams, J. A. G.; Le Bozec, H.; Guerchais, V. *Chem. Commun.* **2008**, 4333.

(3) (a) Eryazici, I.; Moorefield, C. N.; Newkome, G. R. *Chem. Rev.* **2008**, *108*, 1834. (b) Wong, K.M.-C.; Tang, W. S.; Chu, B. W. K.; Zhu, N. Y.; Yam, V. W.-W. *Organometallics* **2004**, *23*, 3459. (c) Ma, D.-L.; Shum, T. Y.-T.; Zhang, F.; Che, C.-M.; Yang, M. *Chem. Commun.* **2005**, 4675. (d) Wu, P.; Wong, E. L.-M.; Ma, D.-L.; Tong, G. S.-M.; Ng, K.-M.; Che, C.-M. *Chem. Eur. J.* **2009**, *15*, 3652. (e) Ma, D. L.; Che, C.-M.; Yan, S.-C. *J. Am. Chem. Soc.* **2009**, *131*, 1835.

(4) (a) Botchway, S. W.; Charnley, M.; Haycock, J. W.; Parker, A. W.; Rochester, D. L.; Weinstein, J. A.; Williams, J. A. G. *Proc. Natl. Acad. Sci. U.S.A.* **2008**, *105*, 16071. (b) Koo, C.-K.; Wong, K.-L.; Man, C. W.-Y.; Lam, Y.-W.; So, K.-Y.; Tam, H.-L.; Tsao, S.-W.; Cheah, K.-W.; Lau, K.-C.; Yang, Y.-Y.; Chen, J.-C.; Lam, M. H.-W. *Inorg. Chem.* **2009**, *48*, 872. (c) Shiu, H.-Y.; Chong, H.-C.; Leung, Y.-C.; Zou, T. T.; Che, C.-M. *Chem. Commun.* **2014**, *50*, 4375. (d) Baggaley, E.; Weinstein, J. A.; Williams, J. A. G. *Coord. Chem. Rev.* **2012**, *256*, 1762. (e) Baggaley, E.; Botchway, S. W.; Haycock, J. W.; Morris, H.; Sazanovich, I. V.; Williams, J. A. G.; Weinstein, J. A. *Chem. Sci.* **2014**, *5*, 879. (f) Guo, Z.; Tong, W. L.; Chan, M. C. W. *Chem. Commun.* **2014**, *50*, 1711.

(5) (a) Balashev, K. P.; Puzyk, M. V.; Kotlyar, V. S.; Kulikova, M. V. *Coord. Chem. Rev.* **1997**, *159*, 109. (b) Brooks, J.; Babayan, Y.; Lamansky, S.; Djurovich, P. I.; Tsyba, I.; Bau, R.; Thompson, M. E. *Inorg. Chem.* **2002**, *41*, 3055. (c) Yin, B. L.; Niemeyer, F.; Williams, J. A. G.; Jiang, J.; Boucekkine, A.; Toupet, L.; Le Bozec, H.; Guerchais, V. *Inorg. Chem.* **2006**, *45*, 8584. (d) Niedermair, F.; Kwon, O.; Zojer, K.; Kappaun, S.; Trimmel, G.; Mereiter, K.; Slugovc, C. *Dalton Trans.* **2008**, 4006. (e) Ghedini, M.; Pugliese, T.; La Deda, M.; Godbert, N.; Aiello, I.; Amati, M.; Belviso, S.; Lelj, F.; Accorsi, G.; Barigelletti, F. *Dalton Trans.* **2008**, 4303. (f) Chang, S.-Y.; Cheng, Y.-M.; Chi, Y.; Lin, Y.-C.; Jiang, C.-M.; Lee, G.-H.; Chou, P.-T. *Dalton Trans.* **2008**, 6901. (g) Liu, J.; Yang, C.-J.; Cao, Q.-Y.; Xu, M.; Wang, J.; Peng, H.-N.; Tan, W.-F.; Lue, X.-X.; Gao, X.-C. *Inorg. Chim. Acta* **2009**, *362*, 575. (h) Santoro, A.; Whitwood, A. C.; Williams, J. A. G.; Kozhevnikov, V. N.; Bruce, D. W. *Chem. Mater.* **2009**, *21*, 3871. (i) Zhou, G.; Wang, Q.; Ho, C.-L.; Wong, W.-Y.; Ma, D.; Wang, L. *Chem. Commun.* **2009**, 3574. (j) Feng, K.; Zuniga, C.; Zhang, Y.-D.; Kim, D.; Barlow, S.; Marder, S. R.; Brédas, J. L.; Weck, M. *Macromolecules* **2009**, *42*, 6855. (k) Zhou, G. J.; Wang, Q.; Wang, X. Z.; Ho, C. L.; Wong, W. Y.; Ma, D. G.; Wang, L. X.; Lin, Z. Y. *J. Mater. Chem.* **2010**, *20*, 7472. (l) Vezzu, D. A. K.; Deaton, J. C.; Jones, J. S.; Bartolotti, L. C.; Harris, F.; Marchetti, A. P.; Kondakova, M.; Pike, R. D.; Huo, S. *Inorg. Chem.* **2010**, *49*, 5107. (m) Wu, W. H.; Wu, W. T.; Ji, S. M.; Guo, H. M.; Song, P.; Han, K. L.; Chi, L. N.; Shao, J. Y.; Zhao, J. Z. *J. Mater. Chem.* **2010**, *20*, 9775. (n) Chan, J. C.-H.; Lam, W. H.; Wong, H.-L.; Zhu, N. Y.; Wong, W.-T.; Yam, V. W.-W. *J. Am. Chem. Soc.* **2011**, *133*, 12690. (o) Turner, E.; Bakken, N.; Li, J. *Inorg. Chem.* **2013**, *52*, 7344. (p) Harris, C. F.; Vezzu, D. A. P.; Bartolotti, L.; Boyle, P. D.; Huo, S. *Inorg. Chem.* **2013**, *52*, 11711.

(6) (a) Williams, J. A. G. *Top. Curr. Chem.* **2007**, *281*, 205. (b) Murphy, L.; Williams, J. A. G. *Top. Organomet. Chem.* **2010**, *28*, 75.

(7) (a) Ballhausen, C. J.; Bjerrum, N.; Dingle, R.; Eriks, K.; Hare, C. R. *Inorg. Chem.* **1965**, *4*, 514. (b) Balzani, V.; Carassiti, V. *J. Phys. Chem.* **1968**, *72*, 383. (c) Andrews, L. J. *J. Phys. Chem.* **1979**, *83*, 3203.

(8) Williams, J. A. G.; Beeby, A.; Davies, E. S.; Weinstein, J. A.; Wilson, C. *Inorg. Chem.* **2003**, *42*, 8609.

(9) Mdleleni, M. M.; Bridgewater, J. S.; Watts, R. J.; Ford, P. C. *Inorg. Chem.* **1995**, *34*, 2334.

(10) Cheung, T. C.; Cheung, K. K.; Peng, S. M.; Che, C. M. *J. Chem. Soc., Dalton Trans.* **1996**, 1645.

(11) (a) Rausch, A. F.; Murphy, L.; Williams, J. A. G.; Yersin, H. *Inorg. Chem.* **2009**, *48*, 11407. (b) Rausch, A. F.; Murphy, L.; Williams, J. A. G.; Yersin, H. *Inorg. Chem.* **2012**, *51*, 312.

(12) (a) Farley, S. J.; Rochester, D. L.; Thompson, A. L.; Howard, J. A. K.; Williams, J. A. G. *Inorg. Chem.* **2005**, *44*, 9690. (b) Develay, S.; Blackburn, O.; Thompson, A. L.; Williams, J. A. G. *Inorg. Chem.* **2008**, *47*, 11129. (c) Williams, J. A. G. *Chem. Soc. Rev.* **2009**, *38*, 1783. (d) Wang, Z.; Turner, E.; Mahoney, V.; Madakuni, S.; Groy, T.; Li, J. *Inorg. Chem.* **2010**, *24*, 11276. (e) Rossi, E.; Murphy, L.; Brothwood, P. L.; Colombo, A.; Dragonetti, C.; Roberto, D.; Ugo, R.; Cocchi, M.; Williams, J. A. G. *J. Mater. Chem.* **2011**, *21*, 15501. (f) Murphy, L.; Brulatti, P.; Fattori, V.; Cocchi, M.; Williams, J. A. G. *Chem. Commun.* **2012**, *48*, 5817. (g) Freeman, G. R.; Williams, J. A. G. *Top. Organomet. Chem.* **2013**, *40*, 89. (h) Nisic, F.; Colombo, A.; Dragonetti, C.; Roberto, D.; Valore, A.; Malicka, J. M.; Cocchi, M.; Freeman, G. R.; Williams, J. A. G. *J. Mater. Chem.* **2014**, *2*, 1791.

(13) (a) Sotoyama, W.; Satoh, T.; Sawatari, N.; Inoue, H. *Appl. Phys. Lett.* **2005**, *86*, 153505. (b) Cocchi, M.; Virgili, D.; Fattori, V.;

Rochester, D. L.; Williams, J. A. G. *Adv. Funct. Mater.* **2007**, *17*, 285. (c) Kalinowski, J.; Cocchi, M.; Virgili, D.; Fattori, V.; Williams, J. A. G. *Adv. Mater.* **2007**, *19*, 4000. (d) Cocchi, M.; Virgili, D.; Fattori, V.; Williams, J. A. G.; Kalinowski, J. *Appl. Phys. Lett.* **2007**, *90*, 023506. (e) Yang, X. H.; Wang, Z. X.; Madakuni, S.; Li, J.; Jabbour, G. E. *Adv. Mater.* **2008**, *20*, 2405. (f) Cocchi, M.; Kalinowski, J.; Murphy, L.; Williams, J. A. G.; Fattori, V. *Org. Electron.* **2010**, *11*, 388. (g) Kalinowski, J.; Cocchi, M.; Murphy, L.; Williams, J. A. G.; Fattori, V. *Chem. Phys.* **2010**, *378*, 47.

(14) Englman, R.; Jortner. *J. Mol. Phys.* **1970**, *18*, 145.

(15) (a) Caspar, J. V.; Kober, E. M.; Sullivan, B. P.; Meyer, T. J. *J. Am. Chem. Soc.* **1982**, *104*, 630. (b) Caspar, J. V.; Meyer, T. J. *J. Phys. Chem.* **1983**, *87*, 952. (c) Kober, E. M.; Caspar, J. V.; Lumpkin, R. S.; Meyer, T. J. *J. Phys. Chem.* **1986**, *90*, 3722.

(16) Whittle, C. E.; Weinstein, J. A.; George, M. W.; Schanze, K. S. *Inorg. Chem.* **2001**, *40*, 4053.

(17) Wilson, J. S.; Chawdhury, N.; Al-Mandhary, M. R. A.; Younus, M.; Khan, M. S.; Raithby, P. R.; Köhler, A.; Friend, R. H. *J. Am. Chem. Soc.* **2001**, *123*, 9412.

(18) (a) Lai, S. W.; Chan, M. C. W.; Cheung, T. C.; Peng, S. M.; Che, C. M. *Inorg. Chem.* **1999**, *38*, 4046. (b) Yam, V. W. W.; Wong, K. M. C.; Zhu, N. *J. Am. Chem. Soc.* **2002**, *124*, 6506. (c) Lu, W.; Chan, M. C. W.; Zhu, N.; Che, C. M.; Li, C.; Hui, Z. *J. Am. Chem. Soc.* **2004**, *126*, 7639. (d) Develay, S.; Williams, J. A. G. *Dalton Trans.* **2008**, 4562. (e) Muñoz-Rodríguez, R.; Buñuel, E.; Williams, J. A. G.; Cárdenas, D. J. *Chem. Commun.* **2012**, *48*, 5980.

(19) (a) Kozhevnikov, V. N.; Durrant, M. C.; Williams, J. A. G. *Inorg. Chem.* **2011**, *50*, 6304. (b) Culham, S.; Lanoë, P.-H.; Whittle, V. L.; Durrant, M. C.; Williams, J. A. G.; Kozhevnikov, V. N. *Inorg. Chem.* **2013**, *52*, 10992.

(20) Rochester, D. L. Ph.D. Thesis, University of Durham, 2007.

(21) Note, however, that the identity of the monodentate ligand can influence solid-state packing and consequently the energy of aggregate emission; e.g.: Rossi, E.; Colombo, A.; Dragonetti, C.; Roberto, D.; Demartin, F.; Cocchi, M.; Brulatti, P.; Fattori, V.; Williams, J. A. G. *Chem. Commun.* **2012**, *48*, 3182.

(22) (a) Chen, Y.; Li, K.; Lu, W.; Chui, S. S.-Y.; Ma, C.-W.; Che, C.-M. *Angew. Chem., Int. Ed.* **2009**, *48*, 9909. (b) Rossi, E.; Colombo, A.; Dragonetti, C.; Roberto, D.; Ugo, R.; Valore, A.; Falciola, L.; Brulatti, P.; Cocchi, M.; Williams, J. A. G. *J. Mater. Chem.* **2012**, *22*, 10650.

(23) (a) Sotoyama, W.; Satoh, T.; Sato, H.; Matsuura, A.; Sawatari, N. *J. Phys. Chem. A* **2005**, *109*, 9760. (b) Rochester, D. L.; Develay, S.; Záliš, S.; Williams, J. A. G. *Dalton Trans.* **2009**, 1728. (c) Tong, G. S.-M.; Che, C. M. *Chem. Eur. J.* **2009**, *15*, 7225.

(24) Lowe, G.; Ross, S. A.; Probert, M.; Cowley, A. *Chem. Commun.* **2001**, 1288.

(25) Hofmann, A.; Dahlenburg, L.; Van Eldik, R. *Inorg. Chem.* **2003**, *42*, 6528.

(26) (a) Zuleta, J. A.; Chesta, C. A.; Eisenberg, R. *J. Am. Chem. Soc.* **1989**, *111*, 8916. (b) Zuleta, J. A.; Bevilacqua, J. M.; Proserpio, D. M.; Harvey, P. D.; Eisenberg, R. *Inorg. Chem.* **1992**, *31*, 2396. (c) Cummings, S. D.; Eisenberg, R. *Inorg. Chem.* **1995**, *34*, 2007. (d) Cummings, S. D.; Eisenberg, R. *J. Am. Chem. Soc.* **1996**, *118*, 1949.

(27) (a) Weinstein, J. A.; Zheligovskaya, N. N.; Mel'nikov, M. Y.; Hartl, F. *J. Chem. Soc., Dalton Trans.* **1998**, 2459. (b) Weinstein, J. A.; Blake, A. J.; Davies, E. S.; Davis, A. L.; George, M. W.; Grills, D. C.; Lileev, I. V.; Maksimov, A. M.; Matousek, P.; Mel'nikov, M. Y.; Parker, A. W.; Platonov, V. E.; Towrie, M.; Wilson, C.; Zheligovskaya, N. N. *Inorg. Chem.* **2003**, *42*, 7077. (c) Weinstein, J. A.; Tierney, M. T.; Davies, E. S.; Base, K.; Robeiro, A. A.; Grinstaff, M. W. *Inorg. Chem.* **2006**, *45*, 4544. (d) Adams, C. J.; Fey, N.; Parfitt, M.; Pope, S. J. A.; Weinstein, J. A. *Dalton Trans.* **2007**, *39*, 4446.

(28) Rakhimov, R. D.; Weinstein, Y. A.; Lileeva, E. V.; Zheligovskaya, N. N.; Mel'nikov, M. Y.; Butin, K. P. *Russ. Chem. Bull.* **2003**, *52*, 1150.

(29) Miller, T. R.; Dance, I. G. *J. Am. Chem. Soc.* **1973**, *95*, 6970.

(30) Li, C. H.; Kui, S. C. F.; Sham, I. H. T.; Chui, S. S. Y.; Che, C.-M. *Eur. J. Inorg. Chem.* **2008**, *15*, 2421.

(31) Yersin, H.; Rausch, A. F.; Czerwieniec, R.; Hofbeck, T.; Fisher, T. *Coord. Chem. Rev.* **2011**, *255*, 2622.

(32) Although the use of λ_{max} will necessarily give an underestimate of the excited state energy, the amount by which it is underestimated should be similar for all complexes within the series, given the similarity in the spectral profiles. Thus, it should not influence the correlation with $\{\ln k_{nr}\}$.

(33) Given that the monomer emission is already deep into the red region of the spectrum, it is possible that any excimer emission, if present, would be in the NIR region and beyond the range of detection available with our instrumentation.

(34) Haas, K. L.; Franz, K. J. *Chem. Rev.* **2009**, *109*, 4921.

(35) Dong, H.; Cheung, S. H.; Liang, Y.; Wang, B.; Ramalingam, R.; Wang, P.; Sun, H.; Cheng, S. H.; Lam, Y. W. *Electrophoresis* **2013**, *34*, 1957.

(36) Amoroso, A. J.; Arthur, R. J.; Coogan, M. P.; Court, J. B.; Fernandez-Moreira, V.; Hayes, A. J.; Lloyd, D.; Millet, C.; Pope, S. J. A. *New J. Chem.* **2008**, *32*, 1097.

(37) Tong, W. L.; Chan, M. C. W.; Yiu, S. M. *Organometallics* **2010**, *29*, 6377.

(38) (a) Kui, S. C. F.; Chow, P. K.; Cheng, G.; Kwok, C. C.; Kwong, C. L.; Low, K. H.; Che, C. M. *Chem. Commun.* **2013**, *49*, 1497. (b) Cheng, G.; Chow, P. K.; Kui, S. C. F.; Kwok, C. C.; Che, C. M. *Adv. Mater.* **2013**, *25*, 6765.

(39) Cárdenas, D. J.; Echavarren, A. M.; Ramírez de Arellano, M. C. *Organometallics* **1999**, *18*, 3337.

(40) Frisch, M. J.; Trucks, G. W.; Schlegel, H. B.; Scuseria, G. E.; Robb, M. A.; Cheeseman, J. R.; Scalmani, G.; Barone, V.; Mennucci, B.; Petersson, G. A.; Nakatsuji, H.; Caricato, M.; Li, X.; Hratchian, H. P.; Izmaylov, A. F.; Bloino, J.; Zheng, G.; Sonnenberg, J. L.; Hada, M.; Ehara, M.; Toyota, K.; Fukuda, R.; Hasegawa, J.; Ishida, M.; Nakajima, T.; Honda, Y.; Kitao, O.; Nakai, H.; Vreven, T.; Montgomery, J. A., Jr.; Peralta, J. E.; Ogliaro, F.; Bearpark, M.; Heyd, J. J.; Brothers, E.; Kudin, K. N.; Staroverov, V. N.; Kobayashi, R.; Normand, J.; Raghavachari, K.; Rendell, A.; Burant, J. C.; Iyengar, S. S.; Tomasi, J.; Cossi, M.; Rega, N.; Millam, J. M.; Klene, M.; Knox, J. E.; Cross, J. B.; Bakken, V.; Adamo, C.; Jaramillo, J.; Gomperts, R.; Stratmann, R. E.; Yazyev, O.; Austin, A. J.; Cammi, R.; Pomelli, C.; Ochterski, J. W.; Martin, R. L.; Morokuma, K.; Zakrzewski, V. G.; Voth, G. A.; Salvador, P.; Dannenberg, J. J.; Dapprich, S.; Daniels, A. D.; Farkas, Ö.; Foresman, J. B.; Ortiz, J. V.; Cioslowski, J.; Fox, D. J. *Gaussian 09W, Version 7.0*; Gaussian, Inc., Wallingford, CT, 2009.

(41) Perdew, J. P.; Burke, K.; Ernzerhof, M. *Phys. Rev. Lett.* **1996**, *77*, 3865.

(42) Adamo, C.; Barone, V. *J. Chem. Phys.* **1999**, *110*, 6158.

(43) Van Houten, J.; Watts, R. J. *J. Am. Chem. Soc.* **1976**, *98*, 4853.

(44) Murphy, L.; Congreve, A.; Palsson, L. O.; Willams, J. A. G. *Chem. Commun.* **2010**, *46*, 8743.